



# Structural, out-gassing and nanomechanical properties of super-hydrophobic transparent silica aerogels developed by ambient pressure drying for space application

MOHAMMED ADNAN HASAN<sup>1</sup>, ARJUN DEY<sup>1,\*</sup> , A CARMEL MARY ESTHER<sup>1,4</sup>,  
PAYEL MAITI<sup>2</sup>, ANOOP KUMAR MUKHOPADHYAY<sup>3</sup> and A RAJENDRA<sup>1</sup>

<sup>1</sup>Thermal Systems Group, U.R. Rao Satellite Centre (formerly ISRO Satellite Centre), Bengaluru 560017, India

<sup>2</sup>Advanced Mechanical and Materials Characterization Division, CSIR - Central Glass and Ceramic Research Institute, Jadavpur, Kolkata 700032, India

<sup>3</sup>Department of Physics, School of Basic Sciences, Faculty of Science, Manipal University Jaipur, Jaipur 303007, India

<sup>4</sup>Present Address: Institute of Materials Physics, University of Munster, Wilhelm-Klemm-Str. 10, 48149 Munster, Germany

\*Author for correspondence (arjun\_dey@rediffmail.com; arjundey@urisc.gov.in)

MS received 15 December 2019; accepted 23 June 2020; published online 29 October 2020

**Abstract.** Transparent super-hydrophobic monolithic silica aerogels are prepared by the cost-effective ambient pressure drying. The drying of aerogel is performed at various temperatures ranging from 25 to 200°C. Oxidation states of different silica aerogels are investigated by XPS which shows the presence of both SiO and SiO<sub>2</sub> phases. Thermal stability of hydrophobic aerogel is found as ~320°C investigated by TGA and DSC. The chemical bonds (i.e., -CH<sub>3</sub>) responsible for the hydrophobic (WCA > 170°) nature of synthesized silica aerogels are identified by FTIR. Further, out-gassing properties of the silica aerogels have been investigated and they are found in limit for the space application. The highest hardness and Young's modulus are measured by the nanoindentation technique for the aerogel dried at 120°C which has higher density, while density decreases for the aerogel dried at 200°C and the corresponding nanomechanical properties are found to be lowest as expected.

**Keywords.** Silica aerogel; hydrophobic; thermal stability; out-gassing; nanoindentation; space application.

## 1. Introduction

Silica aerogels are novel highly porous materials with ultra-low density (e.g., ~0.1 g cm<sup>-3</sup>), large surface area (e.g., ~700 m<sup>2</sup> g<sup>-1</sup>) and very low thermal conductivity (e.g., ~0.02 W m<sup>-1</sup> K<sup>-1</sup>) [1-4]. Therefore, it finds applications in super thermal insulators in space application, waste water treatment, catalytic supports, adsorbents, drug delivery and in many other areas of technological importance [5-13].

The silica aerogel is synthesized by the well-known sol-gel process [14]. Several precursors, such as tetraethyl orthosilicate (TEOS), tetramethyl orthosilicate (TMOS) and sodium silicate (SS) have been reported to be used in development of silica aerogel [2,3,9]. Though, SS is easily available and cost-effective material, but requires repetitive washing during the synthesis process to remove corresponding salt, hence, the total process becomes time-consuming [14,15]. On the other hand, TMOS is identified as toxic compound and the fumes may cause severe illness [16]. In the sol-gel process, first silica gel is obtained by condensation/hydrolysis. TEOS is reported to be

comparatively safer. Then, silica gel is subsequently dried to obtain the aerogel [1,3,17]. Drying process extracts out the solvent present in the pores of the gel. This process leads to the formation of a porous network. Thus, the porous silica aerogel is synthesized. Compared to other methods, such as critical point drying and freeze drying [18,19] which involve high pressures and/or extreme temperatures [15], ambient pressure drying (APD) is adopted in this work because it is simple. But collapse of the pores during drying may lead to fragility during APD. To overcome this problem, usually chemical modification of silica surface needs to be done prior to APD.

In the present work, super-hydrophobic transparent silica aerogels are developed using TEOS precursor by a two-step method [20] followed by APD. It is found that drying temperature plays an important role in determining the properties of synthesized monolithic silica aerogels. Thus, the pore characteristics, structural analysis, thermal stability, out-gassing and nanomechanical properties of super-hydrophobic transparent silica aerogels are presented in the current work. The results appear to have important bearing on a wide variety

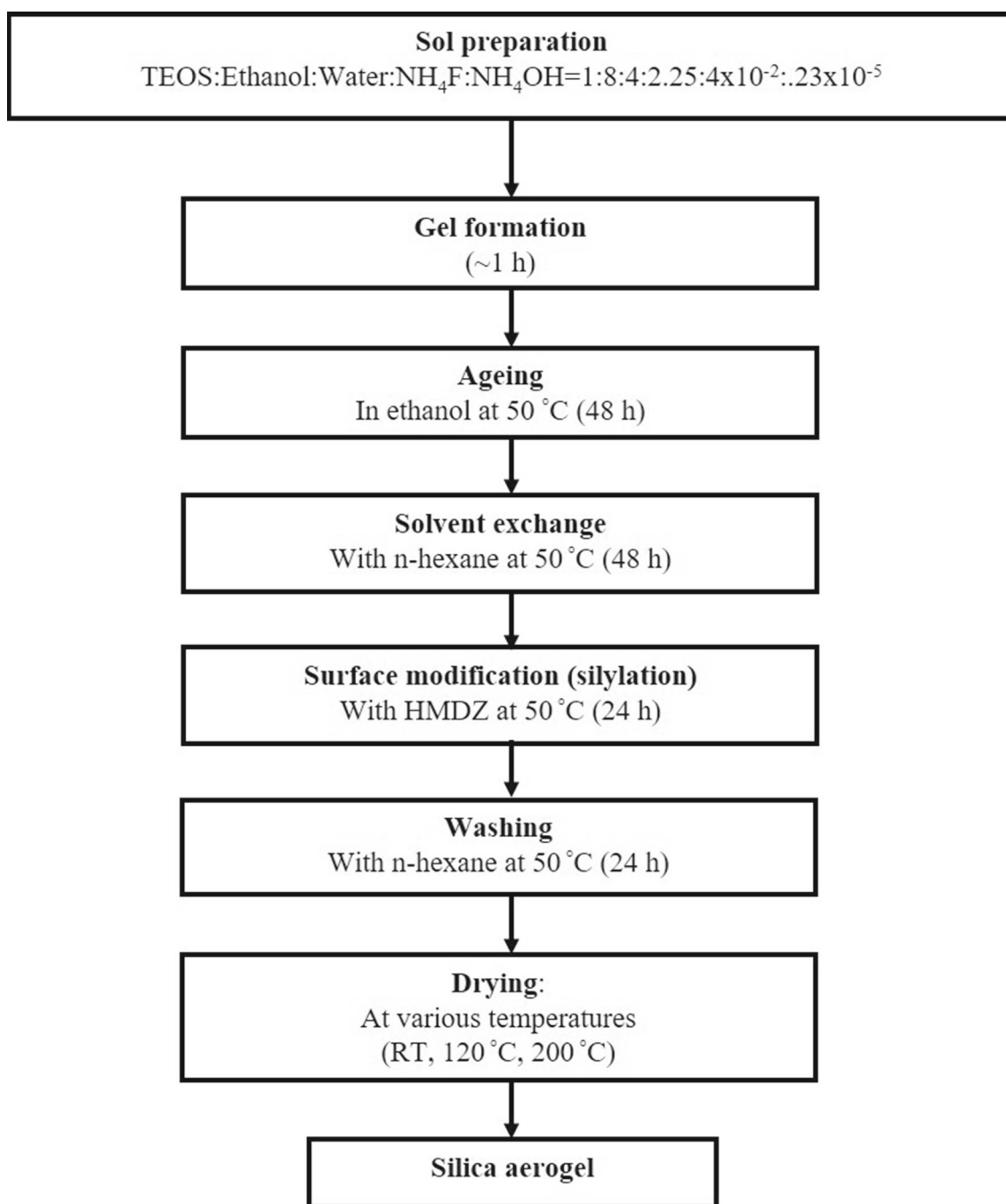


**Figure 1.** Flow chart for synthesis of silica aerogel.

of current and future applications e.g., thermal insulators, structural components, transparent windows, etc. Present aerogel may be suitable also for spacecraft application.

## 2. Materials and methods

### 2.1 Chemicals and precursors

All the chemicals and solvents used in the current work were of analytical reagent (AR) grade. These were

purchased from Merck, Germany. Further, all the chemicals and solvents were used in as-received conditions i.e., without any further purification. TEOS was used as the precursor for silica. Deionized water ( $>18 \text{ M}\Omega \text{ cm}$ , Millipore, USA) was used as reactant. The solvents used were methanol, ethanol and n-hexane. The chemical reaction was accelerated by the catalysts e.g., ammonium fluoride ( $\text{NH}_4\text{F}$ ) and ammonium hydroxide ( $\text{NH}_4\text{OH}$ ,  $\geq 35\%$ ). The surface modification was carried out by hexamethyldisilazane (HMDZ).



**Figure 2.** Typical photographs of transparent silica aerogel developed presently.

## 2.2 Synthesis of aerogel

A two-step sol–gel process, as shown schematically in figure 1, was employed for the synthesis of silica sol. In the first step, TEOS was diluted using ethanol. Then, hydrolysis of diluted TEOS was carried out by adding  $\text{NH}_4\text{F}$  as acidic catalyst. The molar ratio of TEOS: $\text{H}_2\text{O}$  was kept constant at 4. In the second step,  $\text{NH}_4\text{OH}$  was added to the hydrolysis solution as basic catalyst. It was done to start the condensation reaction in the hydrolysed sol. The gel formation takes place within 1 h. After gelation, ageing was performed by immersing the gel in ethanol for 48 h to strengthen the network. Later, ageing solvent present in the pores of gel was exchanged with n-hexane in multiple cycles. After solvent exchange, the silylation was carried out by soaking the alcogel for a period of 24 h in n-hexane containing 10% HMDZ. Following a soak period of 24 h, the alcogels were removed from the soaking mixture. Then, the silylated gels were washed by immersing in hexane for a period of 24 h. In the final step, drying operation was performed to remove the solvent present in the pores of the alcogel. This was done by the low-cost ambient pressure drying method. In this process, the aerogel samples were dried to two different drying temperatures, e.g., 120 and 200°C. Another aerogel sample was kept at room temperature (RT) i.e., ~25°C. The dried hydrophobic transparent silica aerogels were used for characterization studies. Typical optical photographs of the synthesized silica aerogels exhibiting the transparency aspect are shown in figure 2.

## 2.3 Characterizations

The apparent densities of the aerogels were evaluated as a ratio of corresponding mass by volume. The

microstructural characterizations and elemental analysis of the aerogels were performed using field emission scanning electron microscopy (FESEM, Supra VP40 Carl Zeiss, Germany) technique and energy-dispersive X-ray spectroscopy (EDAX, Oxford, UK) facility attached to the same FESEM. The oxidation states of the aerogels were examined by X-ray photoelectron spectroscopy (XPS) analysis (SPECS GmbH, Berlin, Germany) with non-monochromatic  $\text{AlK}\alpha$  radiation (1486.6 eV) as an X-ray source. The chemical bonds of the aerogels were studied by Fourier transform infrared (FTIR, Perkin Elmer, USA) spectroscopy.

The super-hydrophobic characteristic of the aerogels was studied by the semi-automated dynamic water contact angle (WCA) measurement method. A conventional machine (Acam-D2, Apex Instruments Co. Pvt. Ltd., Kolkata, India) was used for this purpose. Accordingly, the automated water dispensing module was set for 10  $\mu\text{l}$  water droplet. The thermal stability of the aerogels was investigated by thermogravimetric analysis (TGA, Q500, TA Instruments, USA) and differential scanning calorimetry (DSC, Q100, TA Instruments, USA). The out-gassing test of the aerogels was conducted according to ASTM E595–93 (ECSS-Q-ST-70-02C) standard. Thus, it required heating the aerogels under a relatively high vacuum of  $5 \times 10^{-5}$  Torr at 125°C in a twin VCM chamber (Balzers, Germany). The nanomechanical characterization was carried out at a low load of 10 mN by using a commercial nanoindenter (Fischerscope H100-XYp, Fischer, Switzerland). The nanohardness ( $H$ ) and Young's modulus ( $E$ ) of the aerogels were evaluated from the experimentally derived load ( $P$ ) vs. depth of penetration ( $h$ ) plots using the well-known Oliver–Pharr method [21]. The loading/unloading time was kept constant at 30 s. To avoid any rate effect, the unloading time was kept the same as the loading time. At least 10 indentations were done in a linear array. The data were represented as the average values of  $H$  and  $E$  derived from the 10 individual nanoindentation experiments. The error bars represent  $\pm 1$  standard deviation.

## 3. Results and discussion

### 3.1 Microstructural analysis

FESEM photomicrographs of the aerogels dried at RT, 120 and 200°C are shown in figure 3a, b and c, respectively. The corresponding EDAX data are shown as insets of figure 3a, b and c, respectively. As expected, microstructures of all the samples are porous. No major microstructural difference is observed for the aerogel samples. The open, porous network structure is because of surface modification by HMDZ. The  $\text{Si-CH}_3$  groups present at the surface reduce capillary stress and result in the formation of porous network [22,23]. The EDAX data confirm the significant presence of Si and O in all the aerogels, as expected.

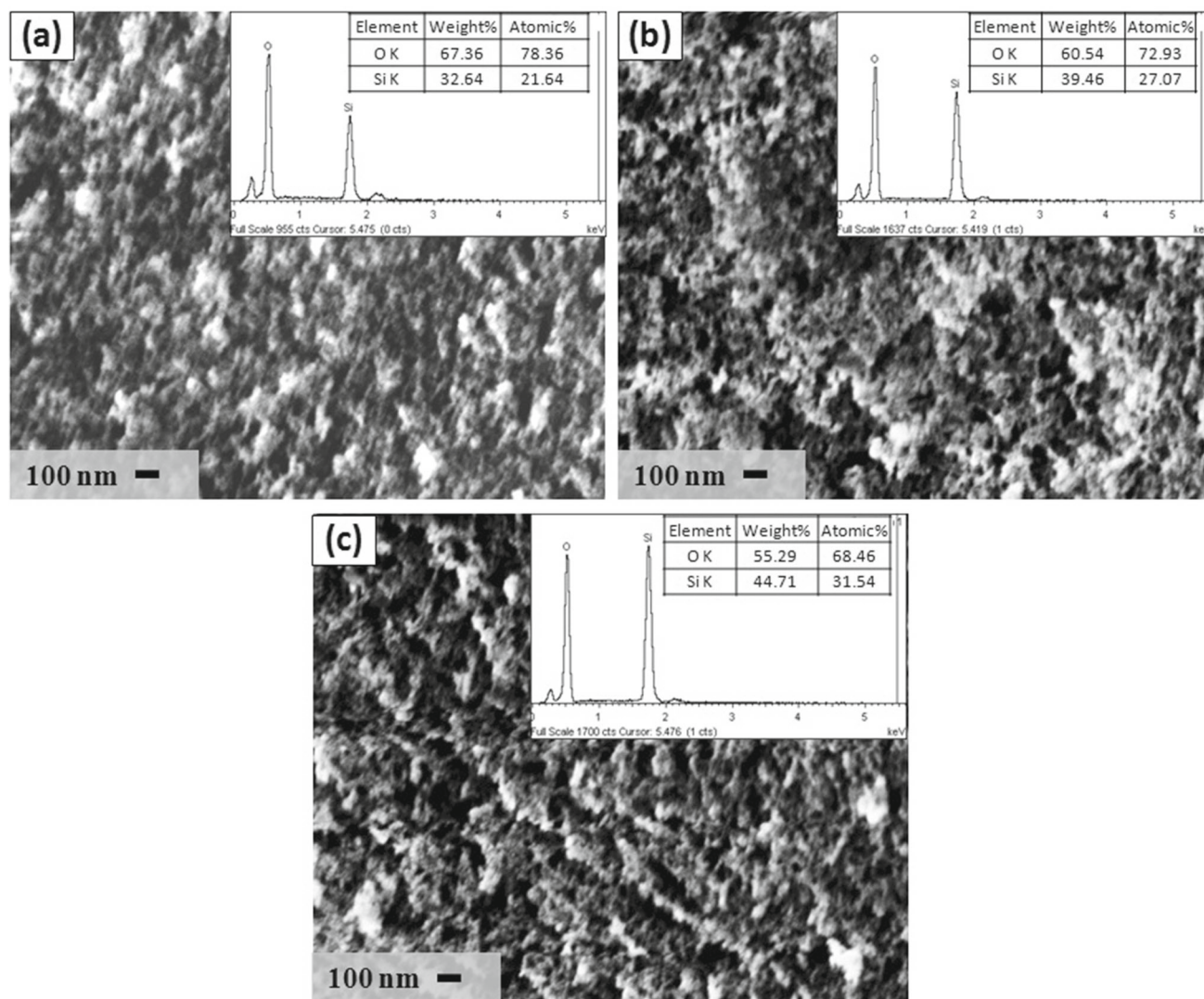


**Figure 3.** FESEM micrographs of transparent silica aerogel dried at (a) RT, (b) 120 and (c) 200°C (insets: corresponding EDAX data).

### 3.2 XPS analysis

XPS survey spectra of the aerogels dried at RT is shown in figure 4a. XPS survey spectra of the aerogels dried at 120 and 200°C are shown in figure 4b and c, respectively. The data from the survey spectra show the expected presence of carbon, oxygen and silicon. The characteristic C1s peak observed at 285 eV in figure 4a–c is due to the carbon atoms present in the  $-\text{CH}_3$  groups used for the modification of the silica surface during processing [24]. The core level XPS spectrum of Si2p of the aerogels dried at RT is shown in figure 5a. The core level XPS spectra of Si2p of the aerogels dried at 120 and 200°C are shown in figure 5b and c, respectively. The Si2p peaks at 102 and 103 eV correspond to the presence of SiO and SiO<sub>2</sub>, respectively [25–27].

### 3.3 FTIR and WCA studies

FTIR spectra of the aerogels dried at RT, 120 and 200°C are shown in figure 6a. For these samples, the detailed FTIR spectra covering the wavenumber range of about 650–1400  $\text{cm}^{-1}$  are given in figure 6b. Further exploded view of the FTIR spectra for these samples in the wavenumber range of  $\sim 2900$ – $3500$   $\text{cm}^{-1}$  are shown in figure 6c. The absorption peaks at  $\sim 1082$ , 740 and 456  $\text{cm}^{-1}$  (figure 6b) are linked respectively, to Si–O–Si asymmetric stretching vibrations, symmetric stretching and deformation vibrations [28,29]. The absorption peaks at near 2962  $\text{cm}^{-1}$  are attributed to stretching vibrations of the terminal  $-\text{CH}_3$  groups. Further, the peaks at 1256, 843 and 750  $\text{cm}^{-1}$  are due to the symmetric deformation vibration and stretching vibration of Si–C bonds [24].

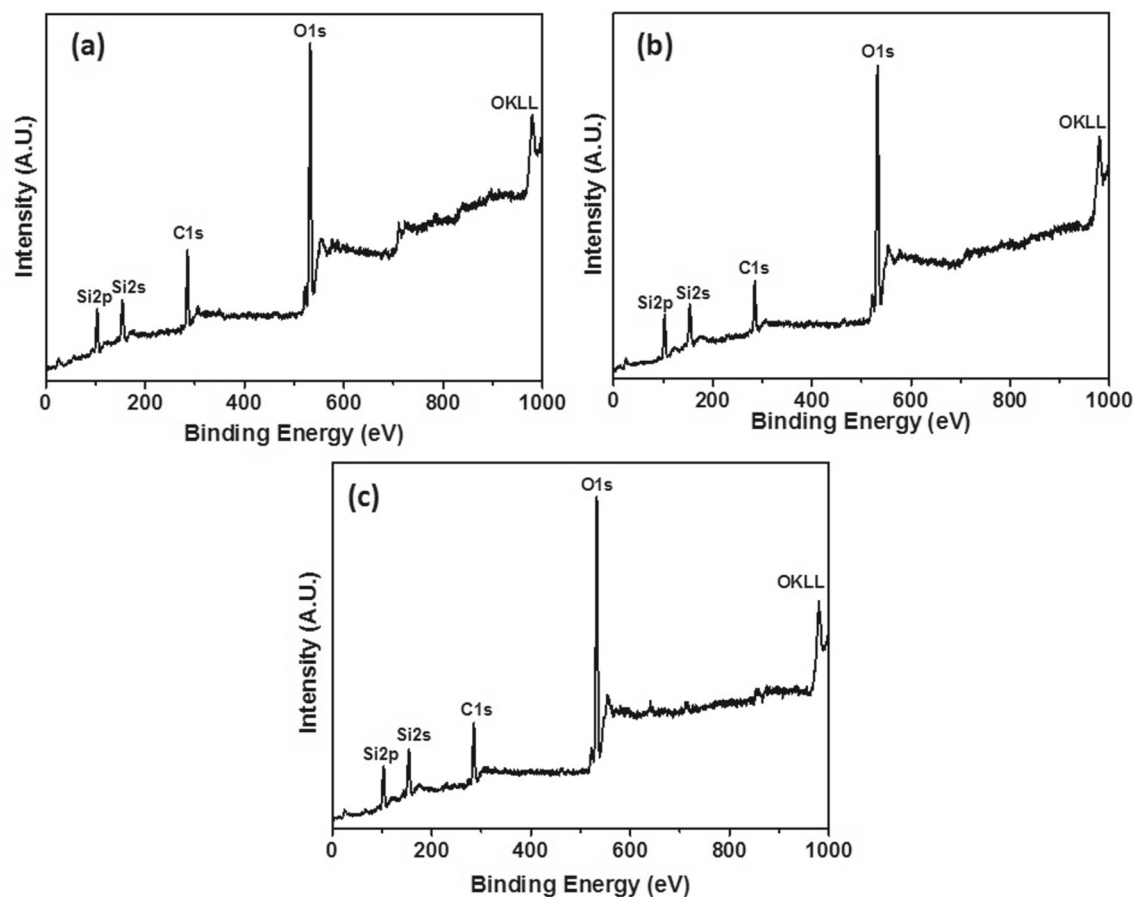


**Figure 4.** XPS survey spectra of transparent silica aerogel dried at (a) RT, (b) 120 and (c) 200°C.

This fact confirms the presence of hydrophobic groups ( $\text{Si-CH}_3$ ) in the present transparent silica aerogel. Due to the presence of the hydrophobic groups ( $\text{Si-CH}_3$ ), the current aerogels exhibit the hydrophobic behaviour. Further, for the silica aerogel dried at 200°C, the increase in peak intensity of the band at  $1082\text{ cm}^{-1}$  is due to the complete formation of  $\text{Si-O-Si}$  bonds.

There are major differences in peak intensities at  $2963$  and  $1082\text{ cm}^{-1}$  for the aerogels dried at different temperatures (figure 6c). Increase in the peak intensity of the band at  $2963\text{ cm}^{-1}$  for the silica aerogel dried at 200°C, shows the formation of more  $\text{CH}_3$  groups at the surface. These  $\text{CH}_3$  groups present at the surface in the silica aerogel dried at 200°C contribute significantly to its hydrophobicity. The optical photograph of WCA measurement of the aerogels dried at RT is shown in figure 7a. For the aerogels dried at 120 and 200°C, the optical photographs of the WCA measurements are shown in figure 7b and c, respectively. These data further confirm the super-hydrophobic nature of all the silica aerogels developed in the current work. However, among all the three of them, the aerogels dried at 200°C is the most hydrophobic (i.e.,  $\text{WCA} > 170^\circ$ ) as shown in figure 7c. This evidence corroborates satisfactorily with the results presented above in figure 6c from the FTIR spectroscopic studies.

### 3.4 Thermal stability studies

TGA data of the aerogels dried at RT, 120 and 200°C are shown in figure 8a. The corresponding DSC data of the aerogels dried at RT, 120 and 200°C are shown in figure 8b. From the TGA plots presented in figure 8a, a negligible weight loss (e.g.,  $< 1\%$ ) is noted to occur at around  $100^\circ\text{C}$ . It happens due to the removal of moisture and adsorbed water from the system. The data plotted in figure 8a also confirm that all silica aerogels are thermally stable up to  $\sim 320^\circ\text{C}$ . Further, DSC data plots (figure 8b) confirm the presence of exothermic peaks in all silica aerogel samples at  $\sim 320^\circ\text{C}$ . It happens due to the oxidation of organic groups and the  $\text{Si-CH}_3$  bonds [30]. Thus, the synthesized transparent aerogels would be hydrophobic up to a temperature of  $\sim 320^\circ\text{C}$ . Beyond this temperature, the aerogels may become hydrophilic due to oxidation of methyl group attached to the silica surface [30].

### 3.5 Out-gassing properties

Our main aim of the present work regarding development of transparent aerogels, are feasibility study towards the space application. In this context, the developed silica aerogels

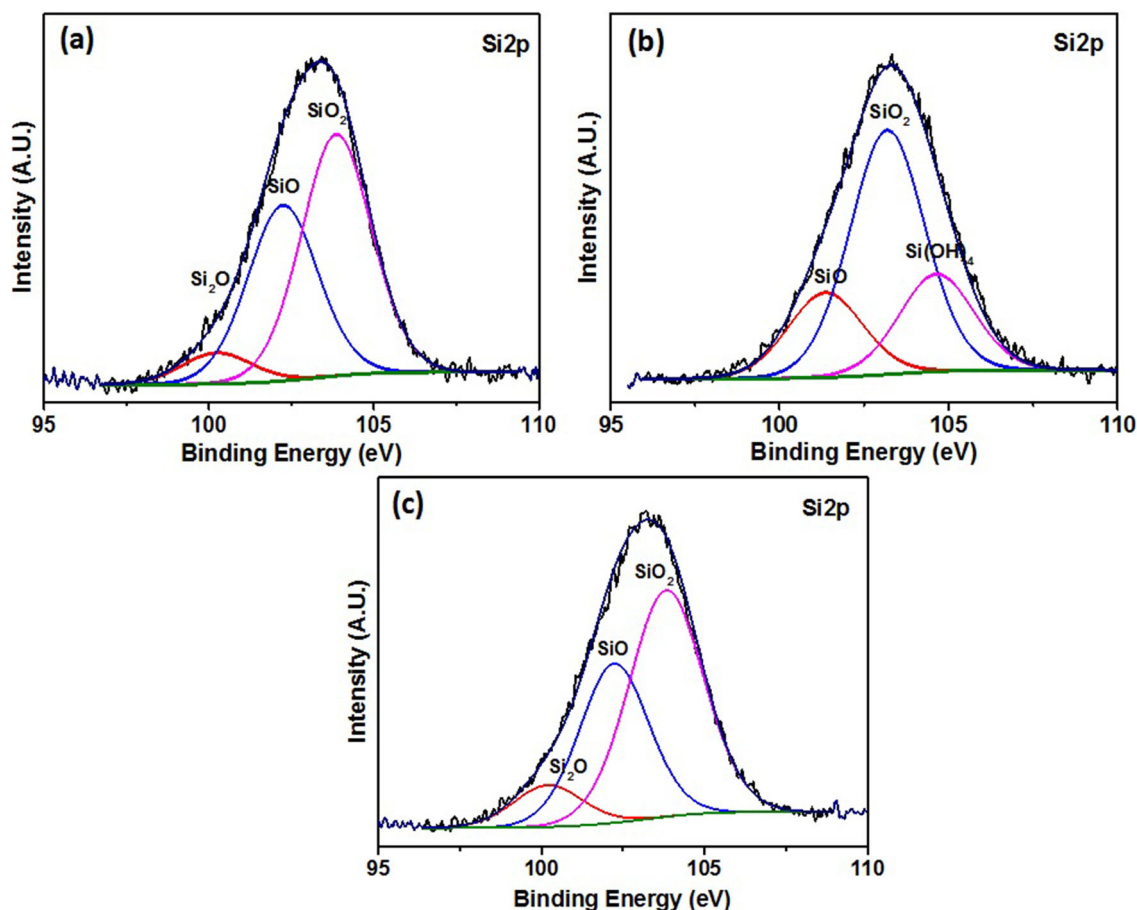


**Figure 5.** XPS spectra of Si2p core levels of transparent silica aerogel dried at (a) RT, (b) 120 and (c) 200°C.

should satisfy the stringent requirements as per recommendation of space agencies. Low out-gassing behaviour is one of the important characteristics which need to be addressed before proposing materials for space applications. In general, out-gassing test measures the amount of slow release of gases and volatile elements from the test coupons/components in simulated space environment. According to the amount of released gases/volatile elements, various properties can be quantified, such as total mass loss (TML), collected volatile condensable materials (CVCM), water vapour regained (WVR) and recovered mass loss (RML). Among them, CVCM is the most important which measures the quantity of volatile materials that are possible to get condensed and may deposit on the nearby other sub-systems or payload's or surfaces. Further, this may cause for altering the thermo-optical and electrical properties of the host surface. Thus, a material with high CVCM is strictly not recommended in spacecraft application.

Out-gassing values of the transparent silica aerogels developed in the present work are presented in table 1. It is observed that TML and WVR for transparent aerogel samples dried at RT and 120°C, are marginally

beyond the limit (i.e., <1%) specified for space applications [31,32]. Slightly higher out-gassing values are due to the presence of organic solvents and physically adsorbed waters in these silica aerogels dried at RT and 120°C. However, volatile materials present in all the current silica aerogels are less condensable. CVCM and RML of all the silica aerogels are well within the space qualification limit of (table 1) which are most important characteristics among other out-gassing properties parameters. But, since the TML and WVR values for the transparent aerogels dried at RT and 120°C are beyond the specified limit of <1%, these materials are suitable for space applications with caution especially the applications near to the optical elements and any other critical payload surfaces. However, the same may be allowed to be used in non-critical place or in enclosed format. The transparent aerogels dried at 200°C show the excellent out-gassing properties as the values of TML, RML, WVR and CVCM are well within the specified limit [31,32], hence, suitable for use in spacecraft application. Further, out-gassing values of the present developed aerogel is similar to the literature reported in this regard [33].

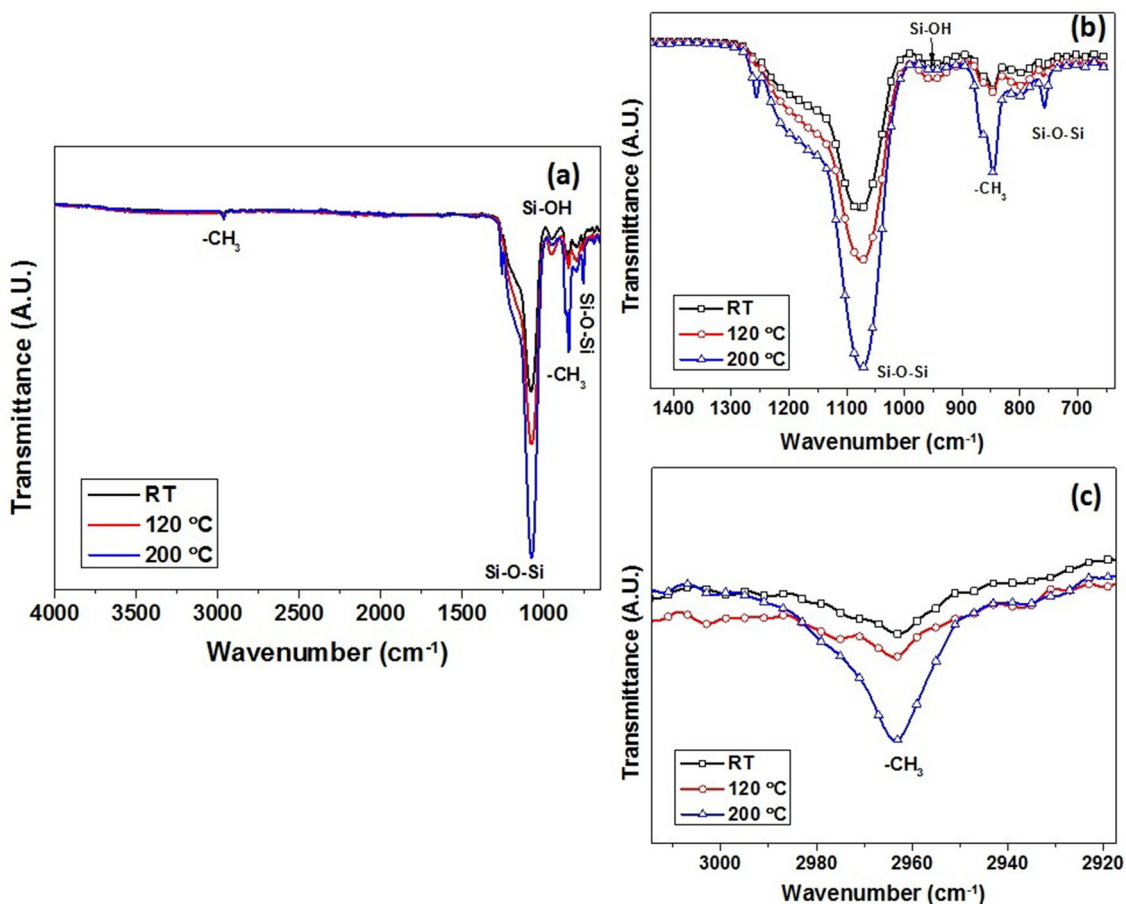


**Figure 6.** FTIR spectra of transparent silica aerogel: (a) full spectra, magnified at (b) Si–O–Si and (c) –CH<sub>3</sub> peak regions.

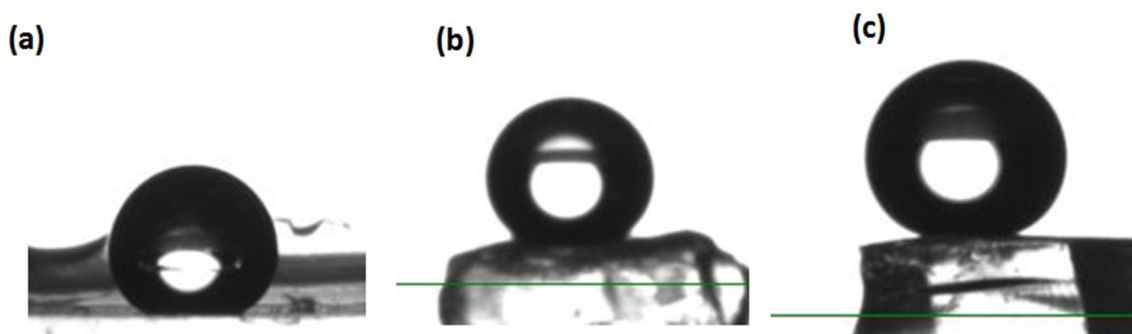


**Figure 7.** Photographs of WCA measurement of transparent silica aerogel dried at (a) RT, (b) 120 and (c) 200°C.

### 3.6 Nanomechanical properties

The *P–h* plots for samples dried at RT, 120 and 200°C is shown in figure 9a. The variations in *H* and *E* data as a function of relative density are shown in figure 9b. The aerogel samples dried at 200°C shows lowest mechanical properties which are believed to be due to lower density. On the other hand, the aerogel dried at 120°C shows significant improvement in density and hence, possesses superior *H* and *E* (figure 9b). Further, nanomechanical properties of

aerogel dried at 120°C is slightly higher than those of the aerogel dried at RT.

### 4. Conclusions

Super-hydrophobic transparent silica aerogels are synthesized in the present work by a cost-effective ambient pressure drying method. The results show that the properties of aerogels are greatly influenced by the drying

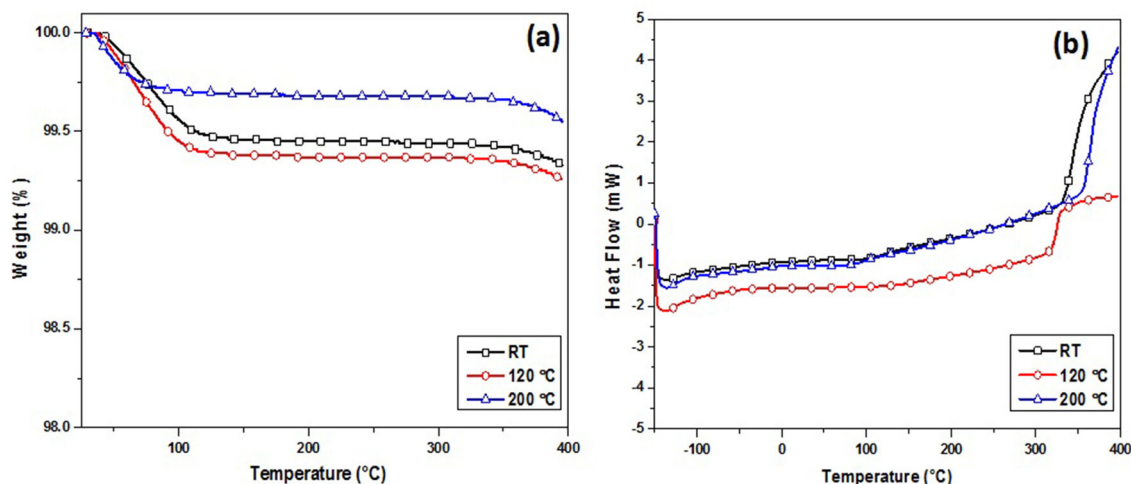


Figure 8. (a) TGA and (b) DSC plots of transparent silica aerogels at different drying temperatures.

Table 1. Out-gassing values of transparent silica aerogel.

Sample	TML (<1%)*	CVCM (<0.1%)*	WVR (<1%)*	RML (<1%)*
Aerogel-RT	2.020	0.006	1.751	0.269
Aerogel-120	1.913	0.007	1.688	0.224
Aerogel-200	0.508	0.008	0.068	0.440

\*Limit for space qualification as per ISRO norms.

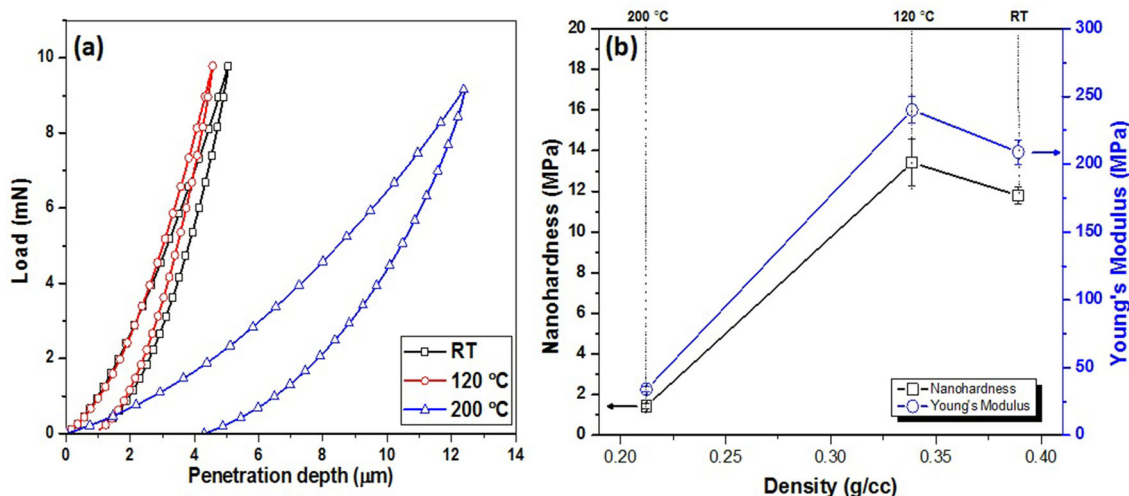


Figure 9. (a) Load vs. depth plots and (b) variations of nanoindentation properties as a function of density of transparent silica aerogels at different drying temperatures.

temperatures. The TGA–DSC analysis shows that due to oxidation of Si–CH<sub>3</sub> to Si–OH groups at around 320°C, the silica aerogels transform from hydrophobic to hydrophilic at about the same temperature. Transparent aerogels dried at 200°C possess super hydrophobicity (i.e., WCA >170°) and excellent out-gassing properties which will confirm its

feasibility to exploit in spacecraft application though it shows comparatively inferior mechanical properties (due to higher porosity). Whereas, aerogels dried at RT and 120° shows superior mechanical behaviour (due to lower porosity) and satisfactory CVCM and RML values, but other out-gassing properties are marginally beyond the specified limit



which would cause restricted uses of them in spacecraft applications.

### Acknowledgements

We acknowledge Mr Siju and Ms Latha from CSIR-NAL, Bengaluru, for carrying out the FESEM and XPS experiments, respectively, under the ISRO rate contract. Further, we are grateful to Mr D R Kumar, URSC/ISRO for facilitating the DSC characterization. Author PM is grateful to Director, CSIR-CGCRI for his kind encouragements, support and permission to publish this work. She also acknowledges the financial support received from INSPIRE Fellowship, Department of Science and Technology, Government of India. One of the authors (AKM) deeply appreciates the kind permissions of Prof G K Prabhu, President and Prof N N Sharma, Pro-President of the Manipal University Jaipur, Rajasthan, India, to publish this work.

### References

- [1] Linhares T, De Amorim M T P and Duraes L 2019 *J. Mater. Chem. A* **7** 22768
- [2] Hasan M A, Sangashetty R, Esther A C M, Patil S B, Sherikar B N and Dey A 2017 *J. Inst. Eng. Ser. D* **98** 297
- [3] Pierre A C and Pajonk M 2002 *Chem. Rev.* **102** 4243
- [4] Kistler S S and Caldwell A G 1934 *Ind. Eng. Chem.* **26** 658
- [5] Du A, Zhou B, Zhang Z and Shen J 2013 *Materials* **6** 941
- [6] Reynolds J G, Coronado P R and Hrubesh L W 2001 *J. Non-Cryst. Solids* **292** 127
- [7] Smirnova I, Suttiruengwong S and Arlt W 2004 *J. Non-Cryst. Solids* **350** 54
- [8] Cuce E, Cuce P M, Wood C J and Riffat S B 2014 *Renew. Sustain. Energy Rev.* **34** 273
- [9] Bheekhun N, Talib A R and Hassan M R 2013 *Adv. Mater. Sci. Eng.* **2013** 18
- [10] Jones S M 2006 *J. Sol-Gel Sci. Technol.* **40** 351
- [11] Kim G S and Hyun S H 2003 *J. Non-Cryst. Solids* **320** 125
- [12] Hrubesh L W 1998 *J. Non-Cryst. Solids* **225** 335
- [13] Schultz J M, Jensen K I and Kristiansen F H 2005 *Sol. Energy Mater. Sol. Cells* **89** 275
- [14] Kistler S S 1931 *Nature* **127** 741
- [15] Bhagat S D, Kim Y, Suh K, Ahn Y, Yeo J-G and Han J H 2008 *Microporous Mesoporous Mater.* **112** 504
- [16] Bhagat S D and Rao A V 2006 *Appl. Surf. Sci.* **252** 4289
- [17] Kistler S S 1932 *J. Phys. Chem.* **36** 52
- [18] Hosticka B, Norris P M, Brenizer J S and Daitch C E 1998 *J. Non-Cryst. Solids* **225** 293
- [19] Bangi U K H, Rao A V and Rao A P 2008 *Sci. Technol. Adv. Mater.* **9** 035006
- [20] Rao A P and Rao A V 2005 *J. Sol-Gel Sci. Technol.* **36** 285
- [21] Oliver W C and Pharr G M 1992 *J. Mater. Res.* **7** 1564
- [22] Shi F, Wang L and Liu J 2006 *Mater. Lett.* **60** 3718
- [23] Dorcheh A S and Abbasi M H 2008 *J. Mater. Process. Technol.* **199** 10
- [24] Bhagat S D, Kim Y, Moon M, Ahn Y and Yeo J 2007 *Solid State Sci.* **9** 628
- [25] Anandan C and Bera P 2013 *Appl. Surf. Sci.* **283** 297
- [26] Lakshmi R V, Bera P, Anandan C and Basu B J 2014 *Appl. Surf. Sci.* **320** 780
- [27] Hasan M A, Dey A, Esther A C M, Sridhara N, Rajendra A and Mukhopadhyay A K 2019 *Int. J. Eng. Sci. Manag.* **1** 77
- [28] Rao A V, Kulkarni M M, Amalnerkar D P and Seth T 2003 *J. Non-Cryst. Solids* **330** 187
- [29] Wei T Y, Chang T F M, Lu S Y and Chang Y C 2007 *J. Am. Ceram. Soc.* **90** 1483
- [30] Yu H, Liang X, Wang J, Wang M and Yang S 2015 *Solid State Sci.* **48** 155
- [31] Campbell W A, Marriott R S and Park J J 1984 *Outgassing data for selecting spacecraft materials*, Volume 1124 of NASA reference publication (National Aeronautics and Space Administration, Scientific and Technical Information Office)
- [32] Hasan M A, Rashmi S, Esther A C M, Bhavanisankar Y, Sherikar B N, Sridhara N et al 2018 *J. Mater. Eng. Perform.* **27** 1265
- [33] Maleki H, Durães L and Portugal A A 2015 *J. Phys. Chem. C* **119** 7689